

## Experimental validation of a finite element model for a heavy impact from the standard rubber ball on a timber floor

Xiaoxue SHEN<sup>1</sup>; Carl HOPKINS<sup>2</sup>;

Acoustics Research Unit, School of Architecture, University of Liverpool, Liverpool, UK

### ABSTRACT

In lightweight buildings there can be problems due to heavy impacts, such as from footsteps in bare feet or children jumping. For this reason the standard rubber ball is used in measurement standards to assess heavy impacts. In this paper, experimental work on a mock-up timber floor is used to provide benchmark data to validate a model using Finite Element Methods (FEM) of the standard rubber ball exciting a timber floor. Experimental Modal Analysis was initially used to extract damping information and the Modal Assurance Criterion was used to confirm that the FEM model of the timber floor was reasonable. A FEM model was then used to predict the time-domain response of the timber floor when excited by a single impact from the standard rubber ball which was included in the FEM model. Comparison of these FEM predictions with experimental data was assessed using the Frequency Domain Assurance Criterion which indicated reasonable agreement with the experimental results.

Keywords: finite element, timber floor, rubber ball

### 1. INTRODUCTION

Heavy impacts on floors in buildings, such as from footsteps in bare feet or children jumping can cause annoyance and disturbance. For this reason, two artificial heavy impact sources, the rubber ball and the bang machine, have been developed to allow field and laboratory measurements (1). The rubber ball is referred to in International measurement standards (2-4) to assess heavy impacts through measurement of the maximum Fast time-weighted sound pressure level,  $L_{Fmax}$ . For heavyweight buildings it is possible to predict  $L_{Fmax}$  using Transient Statistical Energy Analysis (TSEA) (5-8) and with Finite Element Methods (FEM) (9-10). However, for lightweight buildings there are no validated prediction models that can be used to predict the performance in both the laboratory and the field. As the first step in the development of such a model, this paper concerns experimental validation of a FEM model that can predict the vibration response of a small timber floor that is excited by the standard rubber ball.

### 2. TIMBER FLOOR CONSTRUCTION

A free-standing timber floor construction was built that can be isolated from the floor by resilient supports to minimize the influence of a supporting structure on the dynamic response. The floor is comprised of four timber joists (European spruce) at 390 mm spacings and six chipboard sheets with tongue & groove connections between them. In total, 96 metal screws were used to connect the joists along their mid-line to the chipboard; the distance between screws is 180 mm on the same chipboard sheet and 60 mm between those screws at the edge of adjacent chipboard sheets. The properties of the floor components are given in Table 1.

In terms of the boundary conditions, 30 mm thick rubber supports (105 mm × 44 mm) are located underneath both ends of the four joists. The dynamic properties of the rubber were measured to have a spring stiffness of 534,236 N/m and a constant damping ratio of 0.08.

<sup>1</sup> xiaoxue.shen@liverpool.ac.uk

<sup>2</sup> carl.hopkins@liverpool.ac.uk

Table 1 – Timber floor properties

Floor components	Length (m)	Width (m)	Thickness / Depth (m)	Density (kg/m <sup>3</sup> )	Longitudinal wavespeed (m/s)	Young's Modulus (MPa)	Poisson's ratio (-)
Joist 1	3.6	0.044	0.192	468	5060	11.98	0.3
Joist 2				417	4198	7.35	
Joist 3				434	4508	8.82	
Joist 4				432	4652	9.35	
Chipboard	0.6	1.2	0.022	676	2200	3.35	0.3

### 3. EXPERIMENTAL PROCEDURE

#### 3.1 Experimental Modal Analysis

Experimental Modal Analysis (EMA) was carried out on the chipboard surface of the timber floor to identify natural frequencies, mode shapes and modal damping. A force hammer (B&K Type 8200) was used to excite the floor on a rectangular grid of 432 points (100mm separation) with three fixed accelerometer (B&K Type 4371) positions.

The Modal Assurance Criterion (MAC) is used to assess correlation between the EMA and FEM predicted mode shapes using (11)

$$MAC(A, X) = \frac{|\{\psi_X\}^T \{\psi_A\}|^2}{(\{\psi_X\}^T \{\psi_X\})(\{\psi_A\}^T \{\psi_A\})}$$

where  $\psi_X$  and  $\psi_A$  are mode shapes for the experimental and FEM mode shapes respectively, and superscript T indicates the transpose. The experimental mode shapes are complex due to the damping, whereas the FEM mode shapes are real.

#### 3.2 Rubber Ball Excitation

A standard rubber ball (RION) was dropped from a 1m height onto the timber floor. Two excitation positions were identified (see Ref1 and Ref2 on Figure 1); the first is close to the mid-point of the floor between joists and the second is close to a joist. Underneath each of these excitation positions was an accelerometer (B&K Type 4371) which was fixed using cyanoacrylate glue; this formed a reference signal to allow measurement of a complex transfer function for each response point. To measure all response points shown in Fig.1, six accelerometers were used to cover all the 432 sample points in 72 steps. Note that this excluded the two excitation points where the accelerometer was underneath. The FFT frequency span was 1.6k Hz with 3200 FFT lines and a 7 Hz high-pass filter.

The rubber ball was dropped five times at each excitation position to give an average transfer function (in terms of the frequency response function H1) for each response point referenced to the signal underneath the excitation position.

Correlation between the experimental and FEM frequency response functions was assessed using the Frequency Domain Assurance Criterion (FDAC) as given by (11)

$$FDAC(A(\omega_j), X(\omega_i))_k = \frac{|\{H_X(\omega_i)\}_k^T \{H_A(\omega_j)\}_k|^2}{(\{H_X(\omega_i)\}_k^T \{H_X(\omega_i)\}_k)(\{H_A(\omega_j)\}_k^T \{H_A(\omega_j)\}_k)}$$

where  $H_X, H_A$  are the transfer functions of experiment and FE model respectively, and the suffix  $k$  indicates the relevant transfer functions have the  $k^{th}$  sample point as their reference.

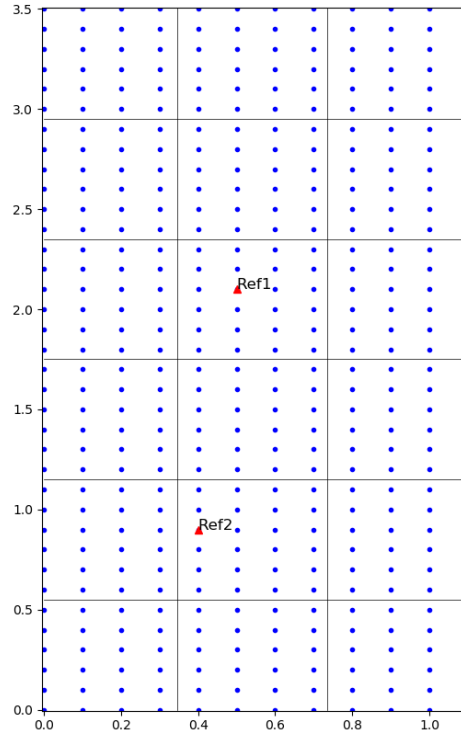


Figure 1 – Sample points and two reference points

## 4. FINITE ELEMENT MODELLING

All finite element modelling was carried out using Abaqus v6.14-2. The undamped natural frequencies and mode shapes were determined using the LANCZOS solver in Abaqus/Standard. The transient response analysis with rubber ball excitation was determined using Abaqus/Explicit. This is a general ‘Hard’ contact applied to the coupling between the rubber ball and the timber floor. The total simulation time is 1s and the fixed time step is  $2 \times 10^{-6}$  s.

### 4.1 Rubber Ball

The rubber ball is modelled as a sphere using a general purpose conventional shell element, S3R (8) with an element size of 15 mm, and shell thickness of 30 mm; this modelling approach was validated in (9-10).

At the time when the rubber ball begins to make contact with the timber floor, a velocity of 4.43 m/s is assigned to the ball to simulate the 1m drop height under gravity. The material properties of the rubber used in the ball were taken from experimentally-derived data from Hirakawa (10); density of  $1188 \text{ kg/m}^3$ , Young’s Modulus of  $3.2 \times 10^6 \text{ N/m}^2$  and Poisson’s ratio of 0.48.

### 4.2 Timber Floor

Both the chipboard and joists are considered as isotropic solids using ‘S4R’ shell elements with an element size of 15 mm. This type of element has six degrees of freedom (dofs) and allows the shell to deform in bending direction. The chipboard is regarded as isotropic because it has nearly the same strain-stress relationship between the two in-plane directions. To simplify the analysis, the timber joists are assumed to be isotropic although wood is typically anisotropic.

Results from Experimental Modal Analysis (EMA) were used to identify the damping of the floor at each mode – see Fig 2. This damping was then applied to both the joists and the chipboard based on a Rayleigh damping model defined by

$$\zeta = \frac{\alpha}{2\omega} + \frac{\omega\beta}{2}$$

where  $\alpha$  is the parameter of mass proportional damping, and  $\beta$  is for stiffness proportional damping. The  $\beta$  term is usually neglected in Abaqus/Explicit because it decreases the stable time increment.

For the 96 screws, a rigid connection “JOIN” is used to join the two nodes with the same position on chipboard and joists, which makes all their active dofs equal. For the tongue and groove structure, the multi-point constraint ‘PIN\_MPC’ is used to provide a pinned joint between two nodes on different chipboard sheets, which makes the displacement equal but leaves the rotations independent of each other. For the interaction between chipboard and joists, the ‘Slide-Plane’ constraint is used to ensure they have the same translation in the normal direction of the chipboard, whilst relative displacements and rotations in other directions are not constrained (8). This is essential to ensure that the joists can only move in the vertical direction.

### 4.3 Boundary Condition

Damped, elastic, 1-D spring connectors are positioned at each of the eight nodes at the end of the joists which sat on the rubber supports. The measured spring stiffness for the material is 534,236 N/m, so each connector is assigned a stiffness of 66,779.5 N/m and a constant damping ratio of 0.08.

## 5. RESULTS

### 5.1 Experimental Modal Analysis

The damping identified in EMA was used to calculate suitable Rayleigh damping for input into the FEM model. As shown in Figure 2, Rayleigh damping using  $\alpha$  and  $\beta$  terms (which can be used in Abaqus Modal Dynamics but is not advisable in Abaqus/Explicit because it decreases the stable time increment) shows better agreement with EMA data above 300Hz; however, in this paper the focus is on the low-frequency performance up to 200Hz for which better agreement is obtained using  $\alpha=37.2$  and  $\beta=0$ .

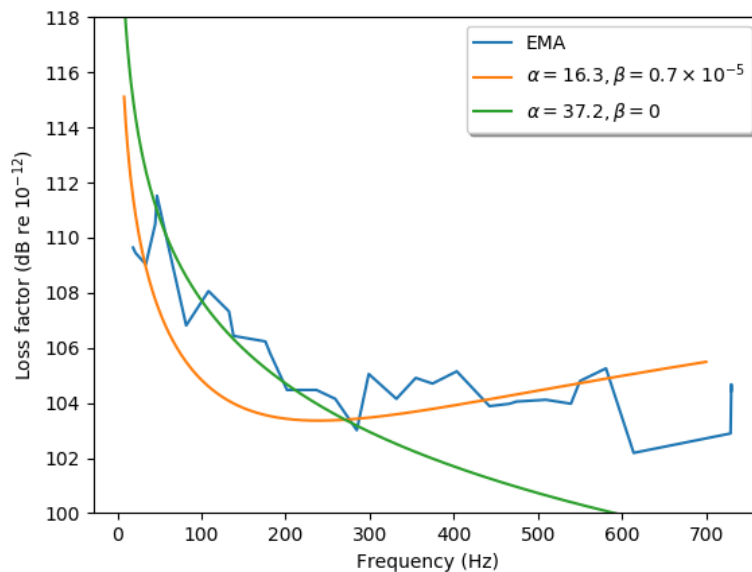


Figure 2 – Comparison of EMA damping and fitted Rayleigh damping curves.

Comparison of the mode frequencies and mode shapes from EMA and FEM is shown in Table 2 for the first 12 modes along with MAC values which are plotted on Figure 3. Apart from two modes, the errors in the mode frequencies are <10% which is reasonable. In terms of MAC, the first three modes are highly correlated and (apart from mode 11) there is reasonable correlation for all the other modes. This agreement was considered sufficient to move on to assess the frequency response functions with rubber ball excitation. However, model updating will be implemented in the future to improve the agreement.

Table 2 – Comparison between EMA and FE results

Modes	EMA (Hz)	FE (Hz)	Error	MAC
1	18.6	20.9	12.4%	0.98
2	21.6	23.7	9.5%	0.96
3	33.8	36.1	6.6%	0.89
4	45.0	45.0	0.1%	0.72
5	47.1	51.5	9.5%	0.67
6	81.8	67.5	17.5%	0.62
7	108.4	109.4	1.0%	0.66
8	132.7	141.5	6.7%	0.79
9	138.1	138.1	0.0%	0.81
10	176.0	169.7	3.6%	0.62
11	181.7	191.3	5.3%	0.42
12	201.7	184.6	8.5%	0.71

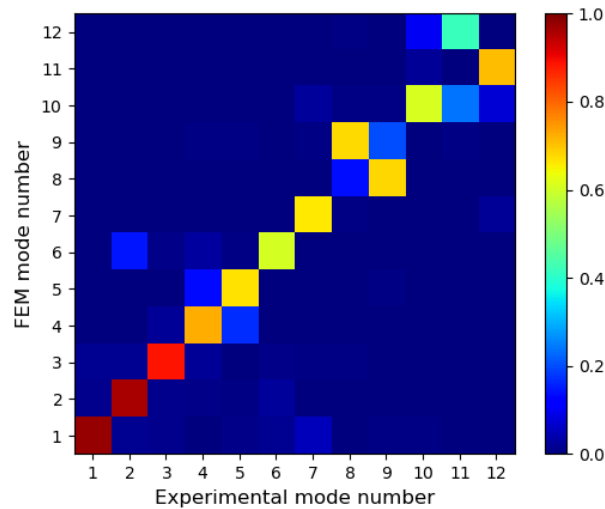


Figure 3 – MAC for EMA and FEM data.

## 5.2 Rubber Ball Excitation

FDAC is calculated for the two reference points and plotted in Figure 4. This shows clear diagonal lines which indicate that the FEM model agrees well with the experimental results below 200 Hz.

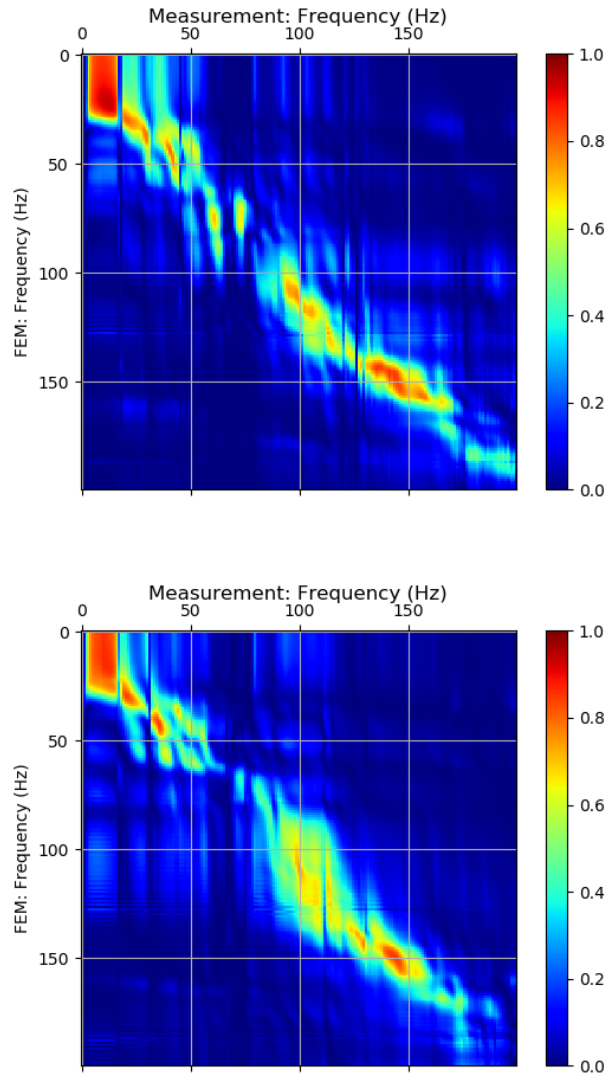


Figure 4 – FDAC for the two excitation points: Ref1 (upper) and Ref2 (lower).

## 6. CONCLUSIONS

In this paper, FEM has been used to model a standard rubber ball impacting a timber floor. Experimental Modal Analysis on the timber floor was initially used to extract damping information and to validate the mode frequencies and mode shapes. A FEM model was then used to predict the time-domain response of the timber floor when excited by a single impact from the standard rubber ball which was included in the FEM model. Comparison of these FEM predictions with experimental data was assessed using the Frequency Domain Assurance Criterion which indicated reasonable agreement with the experimental results. Future work will use model updating to improve the FEM model.

## ACKNOWLEDGEMENTS

This project has received funding from the European Union's Horizon 2020 research and innovation programme under grant agreement No.721536.

The authors are grateful to Dr Gary Seiffert in the ARU for his help with the experimental set-up.

## REFERENCES

1. Tachibana H, Tanaka H, Yasuoka M. and Kimura S. (1998). Development of new heavy and soft impact source for the assessment of floor impact sound insulation of buildings, Proceedings of Internoise 98,

Christchurch, New Zealand.

2. ISO 10140-3:2010+A1:2015. Acoustics – Laboratory measurement of sound insulation of building elements – Part 3: Measurement of impact sound insulation. International Organization for Standardization.
3. ISO 10140-5:2010+A1:2014. Acoustics – Laboratory measurement of sound insulation of building elements – Part 5: Requirements for test facilities and equipment. International Organization for Standardization.
4. ISO 16283-2:2018 Acoustics. Field measurement of sound insulation in buildings and of building elements – Part 2: Impact sound insulation. International Organization for Standardization.
5. Robinson M and Hopkins C. (2014). Prediction of maximum time-weighted sound and vibration levels using transient statistical energy analysis – Part 1: Theory and numerical implementation. *Acta Acustica united with Acustica*, 100(1), 46-56.
6. Robinson M and Hopkins C. (2014). Prediction of maximum time-weighted sound and vibration levels using transient statistical energy analysis – Part 2: Experimental validation. *Acta Acustica united with Acustica*, 100(1), 57-66.
7. Robinson M and Hopkins C. (2015). Prediction of maximum fast time-weighted sound pressure levels due to transient excitation from the rubber ball and human footsteps. *Building and Environment*, 94, 810-820.
8. Hirakawa S and Hopkins C. Experimental determination of transient structure-borne sound power from heavy impact sources on heavyweight floors with floating floors using an inverse form of transient statistical energy analysis. *Applied Acoustics*, 2018;140:74-82.
9. Hirakawa S and Hopkins C. (2018). Prediction of heavy impact sounds using transient statistical energy analysis and finite element methods. *Proceedings of the 25th International Congress on Sound and Vibration 2018, ICSV 2018*, 4377-4383.
10. Hirakawa S. Prediction of impact sound transmission with heavy impact sources in heavyweight buildings. PhD thesis, University of Liverpool (2018).
11. Ewins DJ. *Modal testing: Theory, Practice and Application*. Second Edition. Research Studies Press Ltd. 2000.